Artificial Organs

In Vivo Validation of a Less Invasive Gastrostimulator

*Laurent Lonys, †Anne Vanhoestenberghe, ‡Vincent Huberty, §Martin Hiernaux, *Nicolas Cauche, *Nicolas Julémont, *Adrien Debelle, *François Huberland, *Vicente Acuña, *Carmen Godfraind, ‡Jacques Devière, *Alain Delchambre, *Pierre Mathys, **Stefan Deleuze, and *Antoine Nonclercq

*Bio, Electro and Mechanical Systems Department, Université Libre de Bruxelles, Brussels, Belgium; †Aspire Centre for Rehabilitation Engineering and Assistive Technology, Department of Materials and Tissue, University College London, Stanmore, United Kingdom; ‡Department of Gastroenterology, Hepatopancreatology, and Digestive Oncology, Université Libre de Bruxelles, Erasme University Hospital, Brussels; §Endo Tools Therapeutics SA, Gosselies; and **Département des Sciences Cliniques-Clinique Equine, Université de Liège, Liège, Belgium

Abstract: Gastrointestinal stimulator implants have recently shown promising results in helping obese patients lose weight. However, to place the implant, the patient currently needs to undergo an invasive surgical procedure. We report a less invasive procedure to stimulate the stomach with a gastrostimulator. After attempting fully endoscopic implantation, we more recently focused on a single incision percutaneous procedure. In both cases, the challenges in electronic design of the implant are largely similar. This article covers the work achieved to meet these and details the in vivo validation of a gastrostimulator aimed to be endoscopically placed and anchored to the stomach. **Key Words:** Obesity—Gastric electrical stimulation—Implanted gastric stimulator—Design and implementation—In vivo validation.

Obesity is a pandemic of 21st Century with 2.1 billion overweight adults (body mass index [BMI] above 25) and 600 million obese adults (BMI above 30) worldwide (1–3). Obesity is commonly associated with major health problems, and each year it is responsible for millions of deaths (2–4). Bariatric surgery can be efficient in dealing with this issue but these are invasive operations, performed either by multi-incision laparoscopy or even open surgery. Besides, they represent a large portion of annual healthcare expenditures and are limited to patients whose BMI is over 35 (5). Gastrostimulation has been demonstrated to induce weight loss in humans (6–8). However, current gastrostimulators are bulky and are implanted by multi-incision laparoscopy, a relatively expensive and invasive procedure. Our aims are to develop a new generation of smaller implants, which can be located in a less invasive manner. We have worked on a first design suitable for a fully endoscopic placement, and more recently we have investigated a design for a single-incision laparoscopic procedure. Whatever the chosen implantation solution, the electronic design of these gastrostimulators presents many challenges. From an engineering point of view, compared to currently available stimulators, we aim to:

- reduce the dimensions and weight of the device while protecting it from its environment,
- provide a stable anchoring,
- provide a reliable implantation method to place and attach the device.

This article presents the design and implementation of these novel gastrostimulators. It details the

doi: 10.1111/aor.13056

Received February 2017; revised June 2017; accepted September 2017.

Address correspondence and reprint requests to Laurent Lonys, Université Libre de Bruxelles, BEAMS, Avenue F.D. Roosevelt 50, CP165/56 1050 Brussels, Belgium. E-mail: llonys@ulb.ac.be

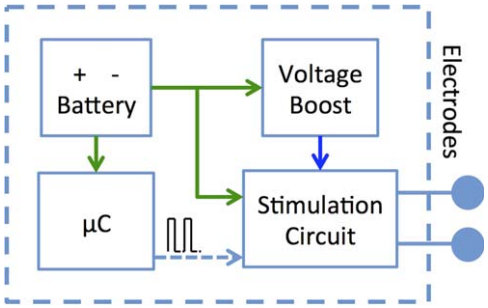

FIG. 1. Block diagram of the implant.

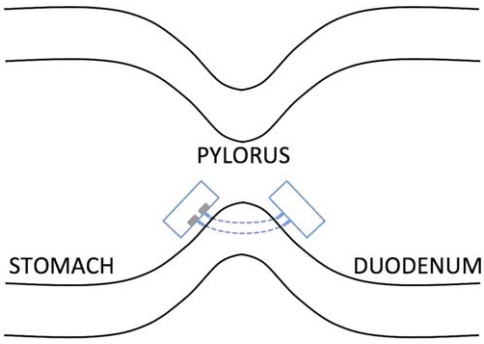

FIG. 2. Anchoring of the implant at the pyloric sphincter.

in vivo validation of a gastrostimulator aimed to be endoscopically implanted. The design and implementation of the gastrostimulator, the test-bench and ex vivo validation have been detailed in a previous publication (9).

MATERIALS AND METHODS

Electronic and mechanical design

The stimulation protocol is based on that of the Enterra device by Medtronic, which has already achieved good results with electrodes near the pylorus in humans (7,8), and at the pylorus in dogs (10). The protocol consists in sending trains of current pulses for 2 s every 5 s. Each train is composed of 5 mA pulses, lasting 330 µs, repeated at 40 Hz. Figure 1 shows a block diagram of our implant, including a non-rechargeable battery, a voltage boost (to feed the stimulator with a voltage higher than the 3.5 V of the battery), a microcontroller µC (for the timing and circuit synchronization) and the stimulation circuit. Briefly, the current source is based upon an operational amplifier driving the gate of a MOS transistor (5LN01) biased in its pinch-off region (i.e., where it behaves like a voltage-controlled current source). A microcontroller (PIC10LF322) is used to switch the amplifier (MAX9911) ON and OFF to obtain the desired stimulation pattern. In this first prototype, power is supplied by a single battery cell whose voltage is too low and varies along the discharge. A voltage boost (LT3464) is used to provide a higher and constant voltage to the stimulation circuit. The battery directly powers the microcontroller and the operational amplifier.

The use of a non-rechargeable battery has been preferred in this work. It allowed the conception of a first prototype, with a battery life sufficient for the first experiments. A button cell (CR2032) suitable for endoscopic implantation in terms of weight (only 2.9 g) and dimensions (20 mm diameter and 3.2 mm height) has been used. Its capacity reaches 220 mAh and its minimum operating voltage fits well those of the op amp, boost, and microcontroller.

We expect in situ impedance ranging from 200 to 800 Ω (11–15). A 2.2 µF blocking capacitor ensures a null mean charge (16). A depletion transistor (LND150) is used to limit the discharge current to at most 20% of the stimulation current. During the stimulation phase, the depletion transistor is blocked and the current goes through the electrodes. During the discharge period, the capacitor discharges through the electrodes (hence the stomach wall) and the depletion transistor.

The circuit fits on a 16-mm diameter substrate. The site of the pyloric sphincter was chosen to anchor the device. The implant is composed of two cylinders linked by a flexible coil. It is designed to be endoscopically placed, with a cylinder on either side of the pylorus. One cylinder hosts the electronics and electrodes to deliver the stimulation (see Fig. 2). The other one contains the battery. Surface recessed electrodes have been chosen to ensure a good contact between the electrodes and the tissue. This also allows a good uniformity of the electric field (17,18). These electrodes are designed to 3 × 3 mm, separated by 2 mm. Their size is based on the available space, choosing them as large as possible to ensure the best contact with the tissue. This also helps to limit the electrode current density and prevents irreversible electro-chemical reactions (19).

Choice of materials

To minimize the device's overall weight and volume, we have opted to protect the electronics by encapsulation (i.e., coating) with silicone rubber. The silicone rubber prevents the circuit from ingress of fluids and protects the body from implant contamination. Silicone encapsulation is used in commercial applications and gives implant lifetimes

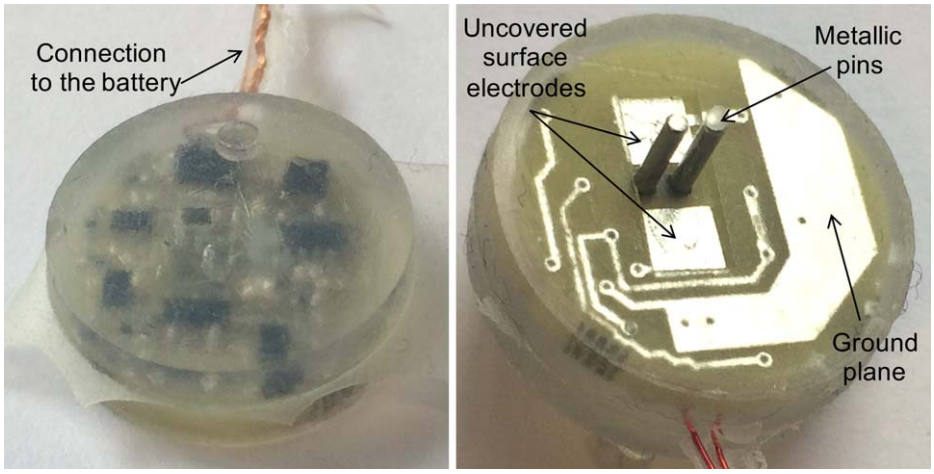

FIG. 3. Illustration of the implant (17 mm diameter and 5.5 mm height) and its two square electrodes.

of several decades (20). It was briefly reviewed by Vanhoestenberghe and Donaldson (21). When the implant is placed in the stomach, this protective layer should resist its acidic environment. This method is well established for human implants (20), but has never been used for devices operating in the stomach, where the very low pH presents a new challenge. The success of this protection relies on the long-term stability of the bond between the encapsulant and the substrate on which the circuit is built (22). Therefore, several couples of substrate and adhesive were tested following Donaldson's method (23).

The long-term stability of the adhesive bond between several couples of substrate and adhesive immersed in simulated gastric liquid was the topic of a previous publication (24). For this animal study, an FR4 substrate was chosen with MED4–4220 silicone rubber (9).

Manufacturing of the implant

The printed circuits were ordered from Eurocircuits. The substrate was made of FR4, and the surface electrodes and electronic tracks were printed in copper.

Cleanliness during the encapsulation process strongly influences the implant's lifetime (22). Briefly, the cleaner the circuit and the substrate, the higher the osmotic gradient, should water vapor, which will rapidly permeate the encapsulation layer, find a condensation site. Liquid water formation would therefore be limited, and what would form would be highly resistive, hence limiting further loss of adhesion and corrosion. Therefore, the devices were thoroughly cleaned using isopropanol and an alkaline cleaning solution, and even more thoroughly rinsed in flowing de-ionized water. A dedicated mold was built to encapsulate the implant. The design of the mold allows a protection layer of silicone rubber of 2 mm on the components side and of 0.5 mm on the other side. The encapsulation was realized using a vacuum centrifuge. The design of the mold allows the 3 × 3 mm surface electrodes to remain uncovered by silicone rubber and hence recessed within a 0.5 mm silicone layer (see Fig. 3). The encapsulated implant, which is 17 mm diameter and 5.5 mm thick, is small enough to allow endoscopic passage through the mouth.

The battery was dip-coated with Dow Corning 3140 silicone rubber and the procedure was repeated until the layer of the silicone rubber was sufficiently thick to cover all the sharp edges. Each new layer of silicone rubber was degassed and dried before the next dip. DC3140 was selected for dip-coating as it forms a thin layer and dries in a few minutes in a humid environment at room temperature. This silicone rubber is, however, not authorized for human implantation. It was used only for this prototyping stage and no adhesion tests were performed between DC3140 and the material of the battery case. Dacron meshes were added to the battery cell helping the surgeon attach the two parts with sutures.

Low temperature gas plasma technology sterilization (Sterrad) was used for the implant and the battery, avoiding a potential degradation of the battery. Steam sterilization was used for all the material not based on silicone rubber, and for the plug connectors to the data acquisition system and the silver electrodes.

Figure 3 shows the resulting implant.

Animal preparation and experimental protocol

Three male beagles were used for this study. The surgical and experimental protocols were approved

by the Animal Care and Use Committee of the Université de Liège.

Dogs were fasted for 24 h before the implantation. They were maintained under general anesthesia with propofol and isoflurane. During the implantation, heart rate and breathing rate of the dogs were monitored.

The procedure aimed to surgically implant in the stomach and validate a gastrostimulator that subsequently could be endoscopically placed and anchored to the stomach. This way, the assessment of the gastrostimulator (stomach stimulation, resistance to stomach environment, anchoring, and noninvasive monitoring) could be performed while eliminating technical difficulties of endoscopic placement.

The implantations lasted between 60 and 90 min. The procedure started with the incision of the cutaneous layer, the muscular aponeurosis, the muscle, and the peritoneum, followed by the dissection of the greater omentum until the pre-pyloric antrum and then the incision of the pylorus. The stimulating part of the implant was first transmurally inserted in the pylorus to reflect the intended position, that is, when the gastrostimulator will be endoscopically placed. During the implantation, the battery cell was considered too cumbersome for implantation in the duodenum and was instead transmurally inserted in the pre-pyloric antrum, to limit the likelihood of bowel obstruction. Before closing the skin, pulses were measured to validate the implant proper position. Then, the surgeon sutured the mucosa and the serosa (i.e., the stomach is sutured), the peritoneum serosa, the muscle layer, and the cutaneous layer (i.e., the skin is sutured). The dogs were returned to their cage right after the implantation, showing no sign of health problems.

To monitor the in vivo activity of the implant, two different methods of measurements were used, with either serosal or cutaneous electrodes. The following material was used:

- an electrophysiological data acquisition system (BIOPAC MP150 data acquisition system), including an electromyogram amplifier (EMG100C);
- cutaneous electrodes (3M EL510);
- homemade 20 mm needle electrodes built from silver wire (ALFA AESAR silver wire, 0.5 mm, 99,9985%).

For both methods of measurements, the data acquisition system was configured to record the propagation of the stimulation pattern (with a 1 Hz–5 kHz bandpass and a 50k sample/s sampling rate). This way, we could assess that the stimulator pulses were properly delivered to the stomach. Please note that we were therefore not focusing at this stage on the physiological effect induced by the stimulation. Before closing the skin, intramuscular data were acquired using the electromyogram amplifier module. Needle electrodes were inserted in the muscular layer, penetrating the serosa near the stimulation site to validate the position of the implant and the contact with the stomach. Recording electrodes were then removed and after closing the skin, the stimulation was recorded using surface electrodes. These electrodes were connected directly to the electromyogram amplifier module. After the day of the implantation (Day D), endoscopies and radioscopies were performed to monitor the implant anchoring and internal response of the dogs.

The monitoring procedure is illustrated in Fig. 4.

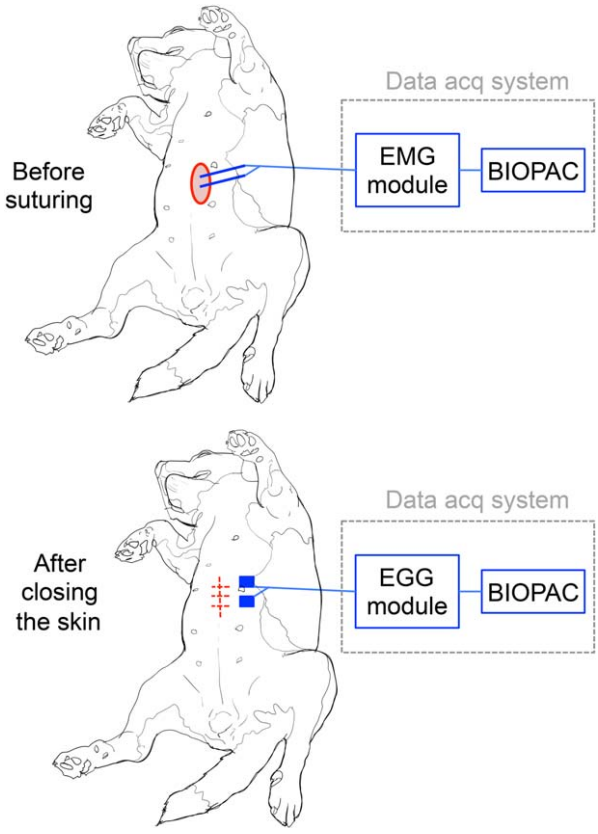

FIG. 4. Two monitoring methods.

RESULTS

The implant main characteristics were first assessed on a test bench and ex vivo before in vivo validation (9).

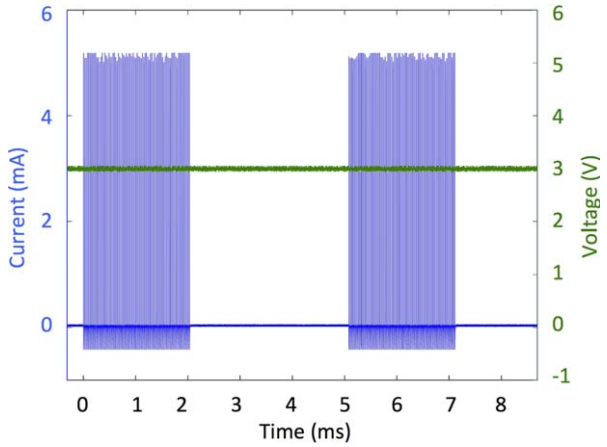

FIG. 5. Monitoring of the pulses train.

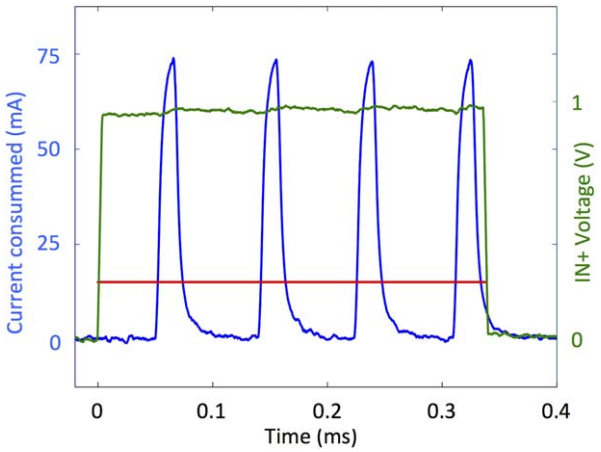

FIG. 6. Current peaks and average current consumed during stimulation: the green curve is the input voltage of the amplifier; the blue curve represents the instantaneous current consumption and red curve is the average current consumption computed over the current peaks.

Stimulation protocol and load range

To validate the stimulation protocol, an implant was used in continuous mode (trains repeated without interruption) with a purely resistive load varying between 200 and 1400 Ω. For load values up to 1200 Ω, we verified that the implant delivered 5 mA pulses, 330 μs wide repeated at 40 Hz and a complete discharge. The trains lasted 2 s and are repeated every 5 s, giving 12 bursts per minute. Figure 5 shows two successive trains of pulses (blue curve) and the power supply voltage (green curve). From 1400 Ω, the stimulation waveform was affected, with lower stimulating current. Also, due to the saturation of the operational amplifier, slightly longer pulses were observed.

Power requirement

The output stage includes a boost DC/DC converter to increase the battery voltage (around 3.3 V) to the 8 V required for the stimulation. The chosen boost (LT3464) uses a discontinuous mode.

1. Output stage consumption (stimulation phase)
   Figure 6 shows that during a stimulation pulse, the instantaneous current from the battery reached peaks of 75 mA, repeated at 11 kHz. The boost was working in a discontinuous mode, as expected. Therefore, during pulse delivery, an average current of 16 mA was drawn from the battery (see red curve on Fig. 6).
2. Output stage consumption (quiet phase)
   Figure 7 shows that in the quiet phase the instantaneous current consumption of the boost also reached peaks up to 75 mA, but only repeated at 20 Hz. This frequency is lower than during a stimulation pulse (11 kHz), since the implant was in quiet phase and hence the current consumption was lower.
3. Implant consumption and lifetime

The total average current of the implant was 370 μA. With an output voltage of 3.5 V (directly measured at the battery output) the battery delivered a power of 1.295 mW. The output voltage and output current of the implant are respectively 8 V and 26 μA, hence the useful power delivered was 208 μW, leading to an efficiency of 16% for the whole system.

The choice of a CR2032 battery cell corresponds to a 27-day lifetime. Note that commercially

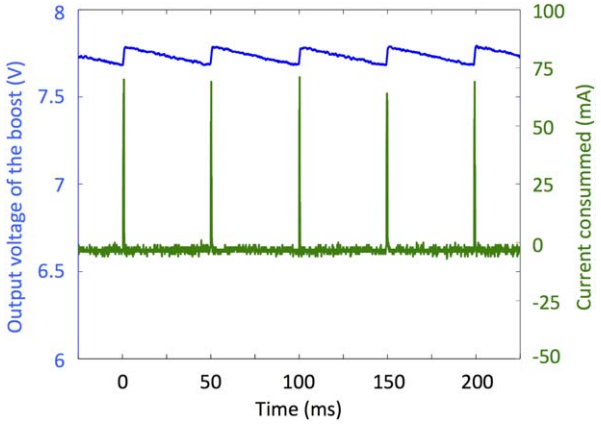

FIG. 7. Output voltage of the boost (blue curve) and current consumption (green curve) during quite phase.

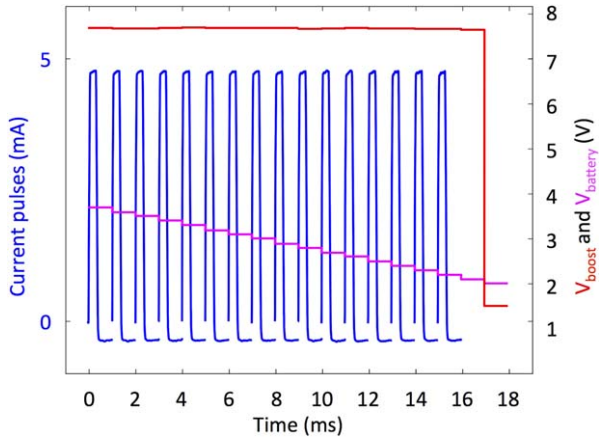

FIG. 8. Effect of the decrease of the battery cell voltage (purple) on the stimulation (blue) and the boost voltage (red).

biocompatible available batteries from EaglePicher, Greatbach, Quallion, and Saft were considered and we found energy densities no higher than 1595 mWh/cm^3. Using this kind of battery, the implant lifetime would reach 51 days per cubic centimeter.

Minimum required voltage

Figure 8 shows the behavior of the implant when the battery voltage decreased due to its discharge. When the battery voltage felt below 2.1 V no pulse was delivered anymore. At 2.1 V, the microcontroller was not able to deliver the desired output values. At 2 V, the boost was no longer working. The implant stopped working without displaying any erratic behavior likely to induce damage.

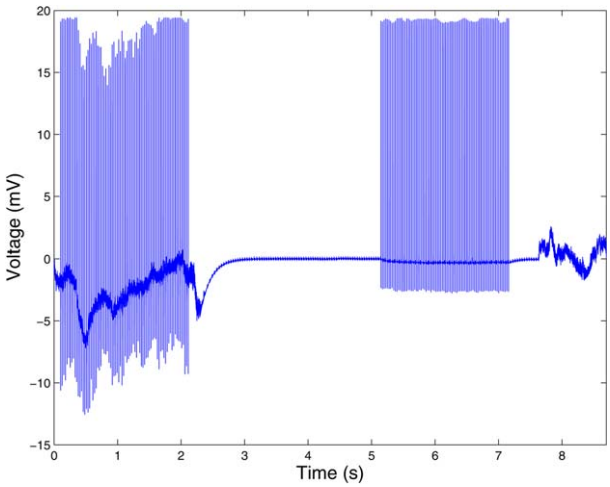

FIG. 9. Serosal measurements of the stimulation on the day of implantation (Day D).

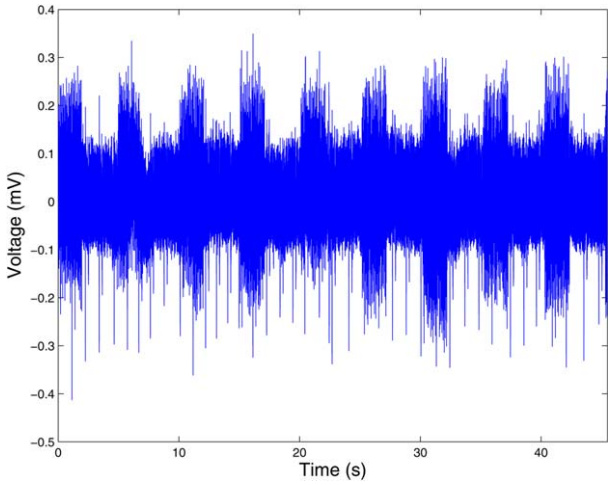

FIG. 10. Cutaneous measurements of the stimulation on the day of implantation (same dog, Day D).

In vivo validation

Three dogs were surgically implanted with the stimulator (Day D) to evaluate its functionality and the propagation of the stimulation. The durability of the anchoring method was also assessed during the experiment.

Figure 9 shows the serosal measurements on the day of the implantation (Day D) in one of the dogs (dog #2). Figure 9 confirms that the stomach was stimulated with trains delivered at the intended frequency. However, the impedance of the tissue could not be verified because of the saturation of the monitoring data acquisition station and the presence of fluid.

Figure 10 shows the cutaneous measurements on the day of the implantation (Day D) in one of the

FIG. 11. Control endoscopy 1 week after the day of implantation (Day D + 7).

TABLE 1. *Schedule of the dogs' follow-ups*

Dog	Day D	D + 1	D + 6	D + 7	D + 10	D + 40
Dog #1	Implantation, Intramuscular measurements, Cutaneous measurements	Radiography	Cutaneous measurements	Radiography, Endoscopy	Radiography	Radiography
Dog #2	Implantation, Intramuscular measurements, Cutaneous measurements	Radiography	Cutaneous measurements	Radiography, Endoscopy	–	–
Dog #3	Implantation, Intramuscular measurements, Cutaneous measurements	Radiography	Cutaneous measurements	Radiography, Endoscopy	–	–

dogs (dog #2). Stimulation was successfully monitored and the intended frequency of the trains was observed.

Figure 11 shows an endoscopic view of the implant in the same dog 1 week after implantation (Day D + 7).

The monitoring was performed as detailed in Table 1. Control postoperative radiographies were performed on Day D + 1 and D + 7 on the three dogs. In the three dogs, radiographies on D + 1 confirm the position of the implant and the battery cell in their initial implantation site. On D + 6, no electrical activity could be measured using cutaneous electrodes in any dogs, indicating either that the implant had stopped stimulating or that it had migrated.

Endoscopies and radiographies performed on D + 7 showed:

- migration in the duodenum of the stimulation part in dog #1 and a potential failure of the electrical wire,
- no migration but a potential failure of the connection between the two parts of the implant in dog #3,
- that the electrical wire came out of its encapsulant on dog #2,

No health problems were detected in dog #2 and dog #3. In dog #1, the stimulating part and the battery cell were retrieved in the stool at D + 12 and D + 42. Post procedure observations of this implant suggest early failure of the adhesion on the side of the ground plane. Early failure could come from the weaker adhesion between silicone rubber and the copper used for the ground plane needed by the boost. The stimulating part of the implant, which was retrieved alone in the stool, was tested after the end of the procedure. It was powered by a regulated supply voltage, but was not operational anymore, meaning no stimulation waveform was observed between the electrodes. Further, no indication of the polarity of the connection to the power supply was available on the implant and this could also have damaged the implant when testing it after the procedure.

DISCUSSION AND CONCLUSIONS

We presented the design and implementation of a gastrostimulator, with reduced dimensions and weight. The device function was first validated on a test bench and ex vivo before in vivo validation in three beagles.

Today, commercial gastrostimulators are derived from the bulky hermetically sealed cardiac pacemakers, hence not allowing endoscopic implantation and durable anchoring at the pylorus. One team has developed an endoscopically implantable gastrostimulator (12). However, they have chosen a voltage stimulator for their design and the device was removed after 2 h in vivo and no information regarding long-term adhesion, or general efficiency of the protection method, could be deduced (12). Our stimulator was specifically designed to stimulate the stomach. The size and weight of the stimulator were designed to allow endoscopic implantation and durable anchoring. A current source was chosen to ensure a controlled stimulating current through the tissue and an adequate couple silicone rubber/substrate was chosen to protect the device from the acidic environment (24). Surface embedded electrodes were able to deliver the stimulation pulses at the intended frequency. The implant is based on discrete commercially available components. A noninvasive recording method was introduced and validated to monitor the functioning of the implant.

The stimulation was successfully monitored using cutaneous electrodes. To the best of our knowledge, this has not been reported in the literature. Other groups have traditionally monitored the response to their implants using endoscopically placed electrodes (25,26).

Our first prototype shows a lifetime of 27 days. Quiescent currents are responsible for a large part of the discharge of the battery. The components

could be—and indeed were in subsequent versions of the implant developed by our group—set in sleep mode during the idle phases. This reduces by half its average consumption and extend the lifetime to 80 days. Yet, other powering solutions are required to reach a long-term treatment and to compete with alternatives such as the gastric balloon. Our team has developed a wireless powering and communication system, able to power an endoscopic implant, and improve its lifetime.

In this work, the electronic circuit of the prototype was supplied by Eurocircuits. It allows fast prototyping with traditional materials for the substrate and the electronic tracks. FR4 with MED4–4220 allows a sufficient lifetime of adhesion for a short-term validation, but for long-term use, FR4 should be replaced by alumina, which offers the longest lifetime with MED4–4220. Further, the encapsulation quality is also influenced by the adhesion with the IC's, the solder, and the copper used for the electronic tracks. A weaker adhesion was, for example, observed between the ground plane and the silicone rubber. Platinum gold could for example replace copper for electronic tracks.

Further work will include the improvement of the connection between the two parts of the implant using a more robust cable, and improving the anchoring method to avoid migration. A new minimally invasive surgical implantation method is also currently under investigation. These implants will include new features such as a wireless communication system. It is of primary importance since it allows to dynamically adapt the stimulation pattern and to monitor the functioning of the implant. The next prototype will therefore be able to stimulate only around mealtime and to prevent the stomach from accommodating to the stimulation. Future tests aim to assess the effect of the gastric stimulation in vivo. Active stimulators will be implanted in dogs to assess the weight loss during stimulation. Different stimulation protocols will be tested during the experiment. The impact on the gastric slow waves, specific hormones, and the amount of food ingested will be monitored to assess the physiological impact of the selected stimulation protocol.

Author Contributions: Laurent Lonys: Design, manufacture and validation of the implant; Anne Vanhoestenberghe: Encapsulation advisor; Vincent Huberty: Medical advisor and endoscopic expert; Martin Hiernaux: Endoscopic anchoring; Nicolas Cauche: Endoscopic anchoring; Nicolas Julémont: Lap-shear experiments; Adrien Debelle: Power electronics; François Huberland: Endoscopic tools; Vicente Acuña: Power electronics; Carmen Godfraind: Wireless powering and communication; Jacques Devière: Medical advisor and endoscopic expert; Alain Delchambre: Scientific expert and advisor; Pierre Mathys: Scientific expert and advisor; Stefan Deleuze: Animal experiments supervisor; Antoine Nonclercq: Supervisor.

REFERENCES

1. Finucane MM, Stevens GA, Cowan MJ, et al. National, regional, and global trends in body-mass index since 1980: systematic analysis of health examination surveys and epidemiological studies with 960 country-years and 9.1 million participants. *Lancet* 2011;377:557–67. doi:10.1016/S0140-6736(10)62037-5.
2. Dobbs R, Sawers C, Thompson F, et al. *Overcoming Obesity: An Initial Economic Analysis*. New York: McKinsey Global Institute, 2014.
3. Ng M, Fleming T, Robinson M, et al. Global, regional, and national prevalence of overweight and obesity in children and adults during 1980 – 2013: a systematic analysis for the Global Burden of Disease Study. *Lancet* 2014;384:766–81. doi:10.1016/S0140-6736(14)60460-8.
4. Drieskens S, Van der Heyden J, Demarest S, Tafforeau J. Is the different time trend (1997–2008) of the obesity prevalence among adults in the three Belgian regions associated with lifestyle changes?. *Arch Public Health* 2014;72:18. doi.org/10.1186/2049–3258-72-18.
5. Weiner JP, Goodwin SM, Chang HY, et al. Impact of bariatric surgery on health care costs of obese persons: a 6-year follow-up of surgical and comparison cohorts using health plan data. *JAMA Surg* 2013;148:555–62. doi:10.1001/jamasurg.2013.1504.
6. Hasler WL. Methods of gastric electrical stimulation and pacing: a review of their benefits and mechanisms of action in gastroparesis and obesity. *Neurogastroenterol Motil* 2009; 21:229–43. doi:10.1111/j.1365-2982.2009.01277.x.
7. Cigaina V. Long-term follow-up of gastric stimulation for obesity: the Mestre 8-year experience. *Obes Surg* 2004; 14(Suppl. 1):S14–22.
8. Shikora SA. "What are the yanks doing?" The US experience with implantable gastric stimulation (IGS) for the treatment of obesity-update on the ongoing clinical trials. *Obes Surg* 2004;14(Suppl. 1):S40–8.
9. Lonys L, Vanhoestenberghe A, Huberty V, et al. Design and implementation of a less invasive gastrostimulator. *Eur J Transl Myol* 2016;26:6019. doi:10.4081/ejtm.2016.6019.
10. Xu X, Zhu H, Chen JDZ. Pyloric electrical stimulation reduces food intake by inhibiting gastric motility in dogs. *Gastroenterology* 2005;128:43–50.
11. Ayinala S, Batista O, Goyal A, et al. Temporary gastric electrical stimulation with orally or PEG-placed electrodes in patients with drug refractory gastroparesis. *Gastrointest Endosc* 2005;61:455–61. http://doi.org/10.1016/S0016-5107(05)00076-3.
12. Deb S, Tang SJ, Abell TL, et al. An endoscopic wireless gastrostimulator (with video). *Gastrointest Endosc* 2012;75: 411–5, 415.e1. http://doi.org/10.1016/j.gie.2011.09.052
13. Elfvin A, Andersson S, Abrahamsson Edebo A, Simrén M, Lönroth H. Percutaneous implantation of gastric electrodes—a novel technique applied in animals and in patients. *Neurogastroenterol Motil* 2007;19:103–9. http://doi.org/10.1111/j.1365-2982.2006.00858.x.
14. Familoni BO, Abell TL, Nemoto D, Voeller G, Johnson B. Electrical Stimulation at a Frequency Higher than Basal Rate in Human Stomach. *Dig Dis Sci* 1997;42:885–91. http://doi.org/10.1023/A:1018804128695.

15. McCallum RW, Lin Z, Forster J, Roeser K, Hou Q, Sarosiek I. Gastric electrical stimulation improves outcomes of patients with gastroparesis for up to 10 years. *Clin Gastroenterol Hepatol* 2011;9:314–9.e1. doi:10.1016/j.cgh.2010.12.013.
16. Nonclercq A, Lonys L, Vanhoestenberghe A, Demosthenous A, Donaldson N. Safety of multi-channel stimulation implants: a single blocking capacitor per channel is not sufficient after single-fault failure. *Med Biol Eng Comput* 2012;50:403–10. doi:10.1007/s11517-012-0889-5.
17. Krueger TB, Stieglitz T, Effects of electrode miniaturization in micromachined neural prostheses. *Proceedings of the 2nd International IEEE EMBS Conference on Neural Engineering*, Institute of Electrical and Electronics Engineers (IEEE). 2005;462–5. http://ieeexplore.ieee.org/lpdocs/epic03/wrapper.htm?arnumber=1419659.
18. Weiland JD, Anderson DJ, Pogatchnik CC, Boogaard JJ, Recessed electrodes formed by laser ablation of Parylene coated, micromachined silicon probes. *Proceedings of the 19th International Conference IEEE/EMBS*, 1997;2273–6.
19. Kane MJ, Breen PP, Quondamatteo F, Olaighin G. BION microstimulators: a case study in the engineering of an electronic implantable medical device. *Med Eng Phys* 2011;33:7–16. http://www.ncbi.nlm.nih.gov/pubmed/21087890.
20. Brindley GS. The first 500 sacral anterior root stimulators: implant failures and their repair. *Paraplegia* 1995;33:5–9. doi:10.1038/sc.1995.3.
21. Vanhoestenberghe A, Donaldson N. The limits of hermeticity test methods for micropackages. *Artif Organs* 2011;35:242–4. http://www.ncbi.nlm.nih.gov/pubmed/21401667.
22. Vanhoestenberghe A, Donaldson N. Corrosion of silicon integrated circuits and lifetime predictions in implantable electronic devices. *J Neural Eng* 2013;10:031002. doi:10.1088/1741-2560/10/3/031002.
23. Donaldson PEK. Aspects of silicone rubber as encapsulant for neurological prostheses. Part 4: two-part rubbers. *Med Biol Eng Comput* 1997;35:283–6.
24. Lonys L, Vanhoestenberghe A, Julémont N, et al. Silicone rubber encapsulation for an endoscopically implantable gastrostimulator. *Med Biol Eng Comput* 2015;53:319–29. http://doi.org/10.1007/s11517-014-1236-9.
25. Daram S, Tang SJ, Abbell T. Temporary gastric electrical stimulation for gastroparesis: endoscopic placement of electrodes (ENDOstim). *Surg Endosc* 2011;25:3444–5. doi:10.1007/s00464-011-1710-5.
26. Xu X, Pasricha PJ, Chen JD. Feasibility of gastric electrical stimulation by use of endoscopically placed electrodes. *Gastrointest Endosc* 2007;66:981–6.